Lessons from the LHC Run 2 on the Nature of the Electroweak Phase Transition and Future Prospects

IFT Seminar

February 6th 2025

Thomas Biekötter

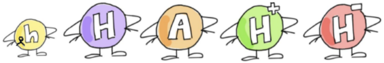

Baryon asymmetry of the universe (BAU)

Baryon-to-photon ratio:

$$\eta = \frac{n_b - n_{\bar{b}}}{n_\gamma} \sim 6 \cdot 10^{-10}$$

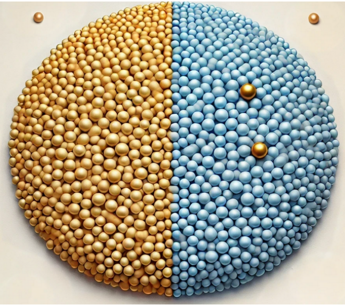

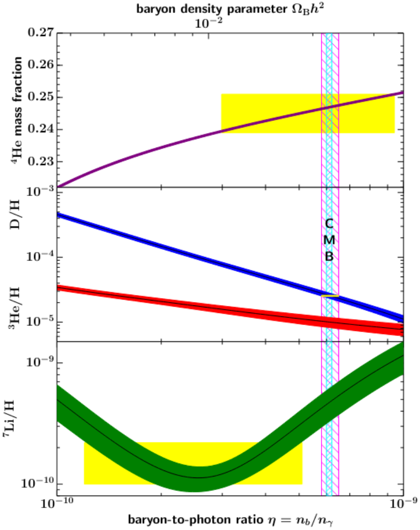

[PDG]

The 3 Sakharov conditions

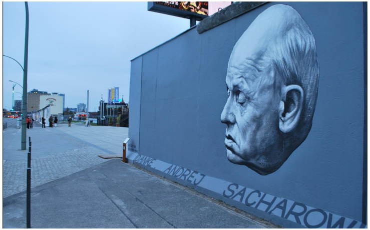

1. Baryon number violation

2. C and CP violation

3. Out of equilibrium

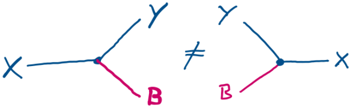

The 3 Sakharov conditions in the SM

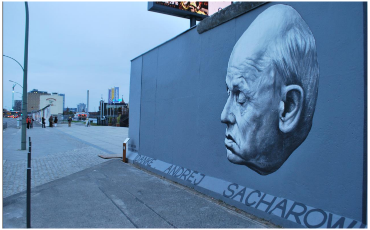

1. Baryon number violation ✓

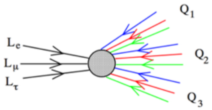

Sphaleron process, active at $T \gtrsim v$

[Klinkhammer et al. (1984), Kuzmin et al. (1985)]

2. C and CP violation (✗)

CP violation from CKM:

$$\Rightarrow \eta \sim 10^{-20}$$

(assuming strong EWPT)

[Gavela et al, hep-ph/9312215]

3. Out of equilibrium ✗

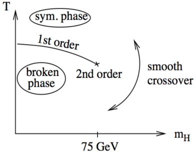

"...there is no EWPT in the SM."

[Rummukainen et al, hep-lat/9805013]

Cosmological phase transitions

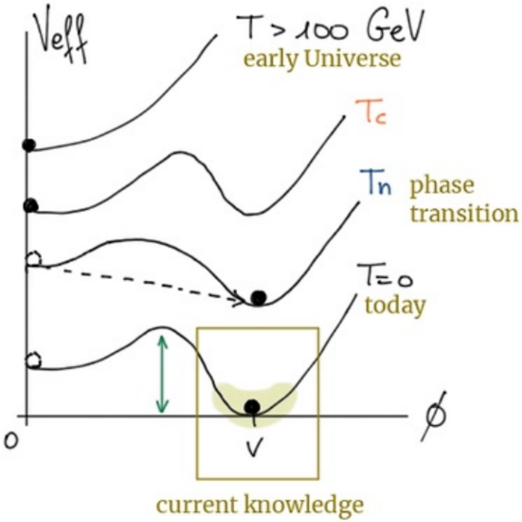

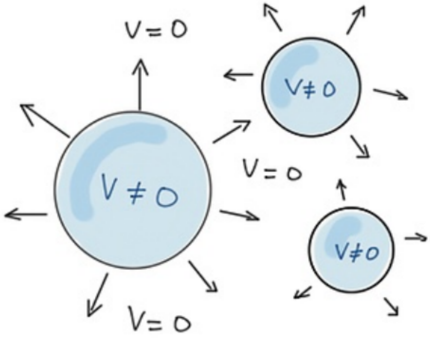

[Kateryna Radchenko]

EW baryogenesis

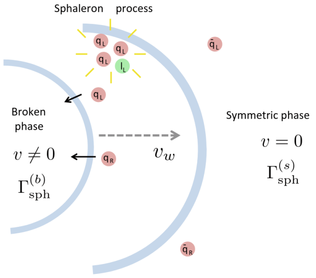

[K. Fuyuto, PhD thesis]

Outside the bubbles: Quantum mechanical sphaleron processes create the B-asymmetry
Inside the bubbles: Sphalerons must be suppressed.

S.Dimopoulos, L. Susskind, Phys.Rev.D 18 (1978) 4500-4509:

> events are really important. The point is that the rates for these processes are of the renormalizable type for T>250 GeV. Thus they can allow the system to return to equilibrium and may wash out any excess which developed at super high temperature.

Condition to prevent the washout of the asymmetry: $\dfrac{v}{T} \gtrsim 1$

$\rightarrow$ Strong 1st-order phase transition [Kuzmin, Rubakov, Shaposhnikov, Phys.Lett.B 155 (1985) 36]

Gravitational waves from the very^2 early universe

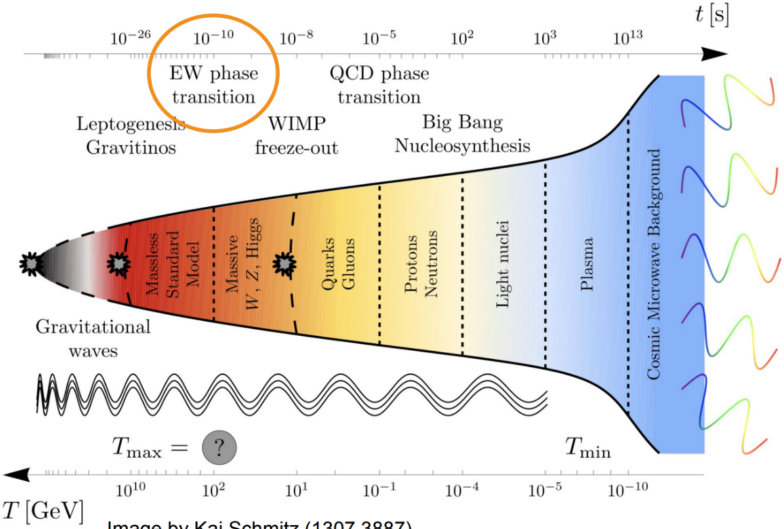

Image by Kai Schmitz (1307.3887)

Types of EWPTs

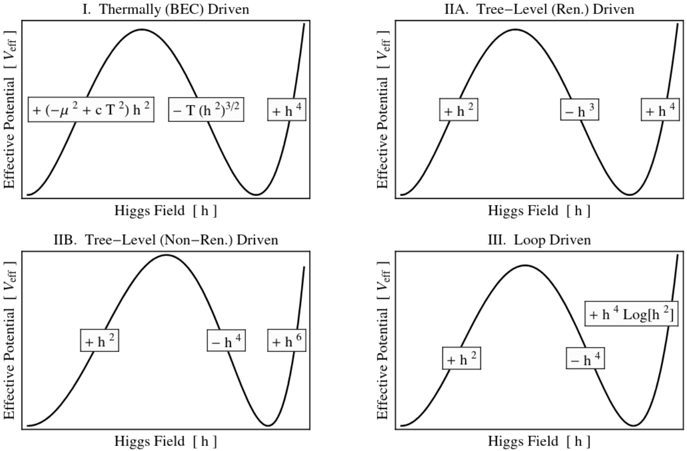

[Chung et al, hep-ph/1209.1819]

Types of EWPTs

e.g. $\mathrm{SM}_{m_h \lesssim 60\ \mathrm{GeV}}$

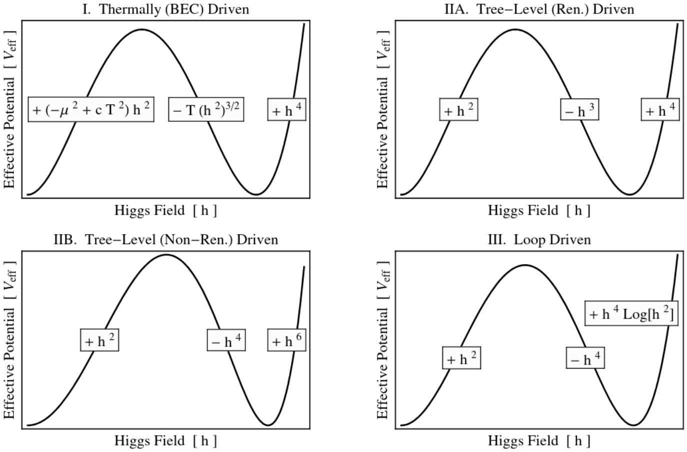

[Chung et al, hep-ph/1209.1819]

Types of EWPTs

e.g. $\mathrm{SM}_{m_h < 60\ \mathrm{GeV}}$

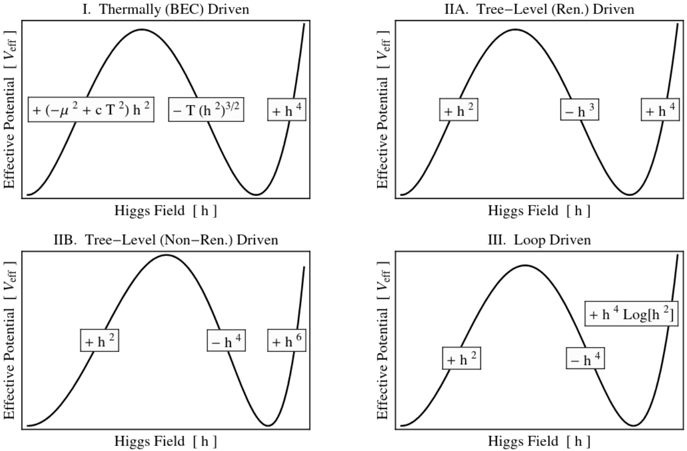

e.g. SM + singlet

[Chung et al, hep-ph/1209.1819]

Types of EWPTs

e.g. $\mathrm{SM}_{m_h<60\ \mathrm{GeV}}$

e.g. SM + singlet

e.g. SMEFT

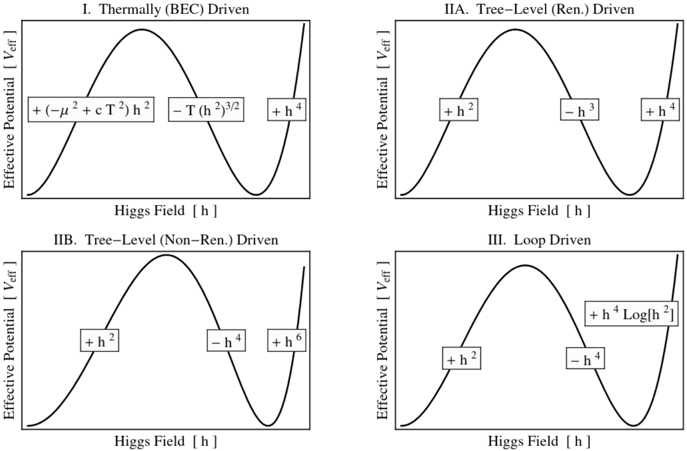

[Chung et al, hep-ph/1209.1819]

Types of EWPTs

e.g. $SM_{m_h < 60\ \mathrm{GeV}}$

e.g. SM + singlet

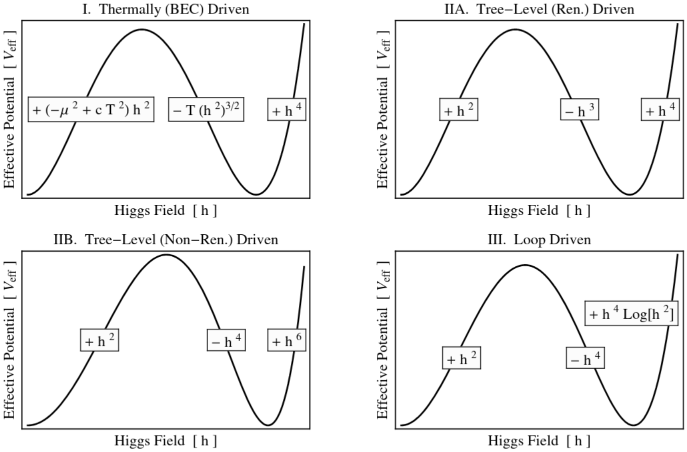

e.g. SMEFT

e.g. 2HDM

[Chung et al, hep-ph/1209.1819]

Nature is typically more complicated

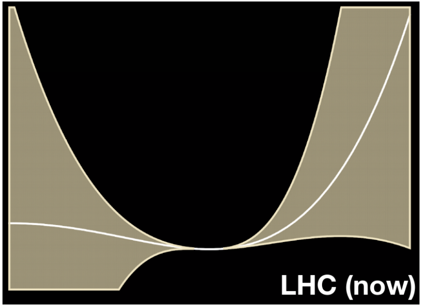

[N. Craig]

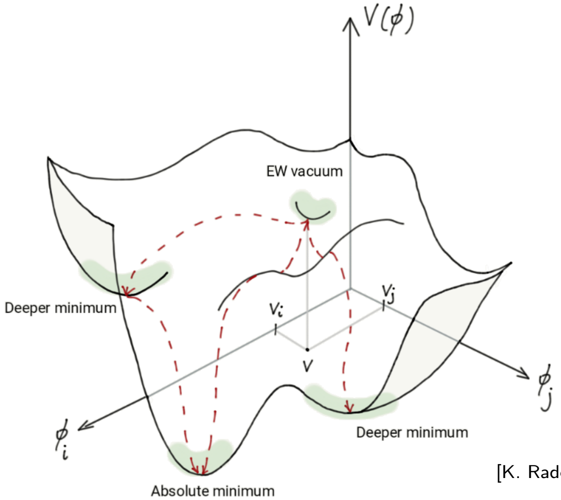

[K. Radchenko]

Experimental landscape: EW baryogenesis can be tested

The Higgs potential has to be significantly modified to facilitate an EWPT

Collider target: new physics at TeV scale

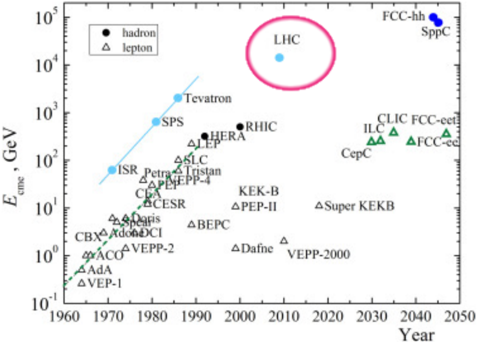

[Gray (2021)]

GW astronomy: $T_n \sim 100$ GeV $\to f_{\rm peak} \sim 1$ mHz

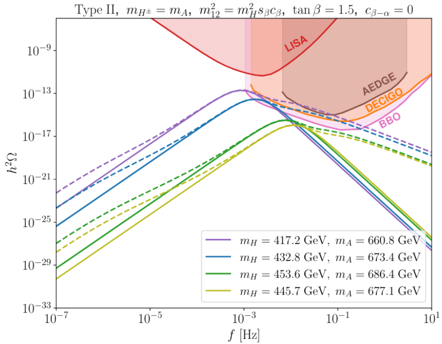

[TB, Heinemeyer, Olea-Romacho, No, Radchenko, Weiglein, 2309.17431]

Other phenomenological consequences: primordial black holes, primordial magnetic fields, particle production

The two Higgs doublet model (2HDM)

(One of) the simplest model for EW baryogenesis: SM + second Higgs doublet

$$V_{\text{tree}} = m_{11}^2 |\Phi_1|^2 + m_{22}^2 |\Phi_2|^2 - m_{12}^2 \left(\Phi_1^\dagger \Phi_2 + \text{h.c.}\right) + \frac{\lambda_1}{2} \left(\Phi_1^\dagger \Phi_1\right)^2 + \frac{\lambda_2}{2} \left(\Phi_2^\dagger \Phi_2\right)^2$$
$$+ \lambda_3 \left(\Phi_1^\dagger \Phi_1\right)\left(\Phi_2^\dagger \Phi_2\right) + \lambda_4 \left(\Phi_1^\dagger \Phi_2\right)\left(\Phi_2^\dagger \Phi_1\right) + \frac{\lambda_5}{2}\left[\left(\Phi_1^\dagger \Phi_2\right)^2 + \text{h.c.}\right]$$

Softly-broken $\mathbb{Z}_2$ symmetry $(\Phi_1 \to \Phi_1, \Phi_2 \to -\Phi_2)$ to avoid FCNC

$\to$ Yukawa types I, II (=Susy), lepton-specific/III, flipped/IV

EW vacuum:

$$\langle \Phi_1 \rangle = \begin{pmatrix} 0 \\ v_1 \end{pmatrix} \qquad \langle \Phi_2 \rangle = \begin{pmatrix} 0 \\ v_2 \end{pmatrix}$$

[Image by K. Radchenko]

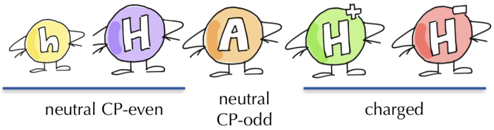

Free parameters: $m_h = 125$ GeV, m_H, m_A, $m_{H^\pm}$, m_{12}^2, $v = \sqrt{v_1^2 + v_2^2} = 246$ GeV, $\tan\beta = \frac{v_2}{v_1}$, α

The 2HDM at finite temperature

$$V_{\text{eff}} = \underbrace{V_{\text{tree}}(\phi_i) + V_{\text{CW}}(\phi_i) + V_{\text{CT}}(\phi_i) + V_{\text{T}}(\phi_i, T)}_{\text{tree-level + one-loop}} \quad \underbrace{+V_{\text{daisy}}(\phi_i, T)}_{\text{resummed n-loop daisy diagrams}}$$

V_{tree}: Classical (tree-level) potential

V_{CW}: One-loop radiative corrections (at $T = 0$) [S. R. Coleman, E. J. Weinberg (1973)]

V_{CT}: UV-finite counterterm potential (OS conditions) [Basler, Mühlleitner, 1803.02846]

V_{T}: One-loop thermal corrections · [L. Dolan, R. Jackiw (1974)]

V_{daisy}: Resummation of daisy diagrams [P. Arnold, O. Espinosa (1996)]

$$V_{\text{CW}}(\phi_i) = \sum_j \frac{n_j}{64\pi^2} (-1)^{2s_i}\, m_j^4(\phi_i) \left[\ln\left(\frac{|m_j(\phi_i)^2|}{\mu^2} \right) - c_j \right]$$

$$V_T(\phi_i) = \sum_j \frac{n_j\, T^4}{2\pi^2} J_\pm\left(\frac{m_j^2(\phi_i)}{T^2} \right)$$

$$V_{\text{daisy}}(\phi_i) = -\sum_k \frac{T}{12\pi} \left(\left(\bar{m}_k^2(\phi_i, T) \right)^{\frac{3}{2}} - \left(m_k^2(\phi_i) \right)^{\frac{3}{2}} \right)$$

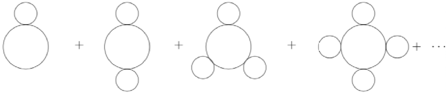

Daisy diagrams

[More details: M.Quiros, hep-ph/9901312]

More precise predictions using 3D EFTs

Predictions for GW signals require an improved theoretical description of the EWPT
$\rightarrow$ dimensionally reduced EFTs [Farakos et al, 9404201], [Ekstedt et al, 2205.08815]

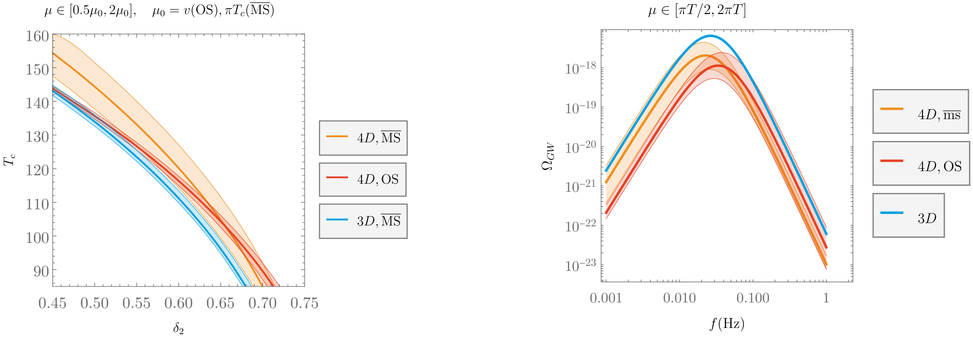

[TB, A. Dashko, M. Löschner, G. Weiglein, tbp]

This is ongoing work. Results shown in this talk are based on the “traditional” 4D approach

2HDM Higgs-boson spectrum

Decoupling limit:

$M = m_H = m_A = m_{H^\pm}$

mass splitting unconstrained $\Longrightarrow$ No EWPT

$m_h = 125$ GeV

+ alignment limit: $\alpha = \beta$

$\rightarrow \cos(\beta - \alpha) = 0$

2HDM Higgs-boson spectrum

Non-decoupling scenarios for an EWPT:

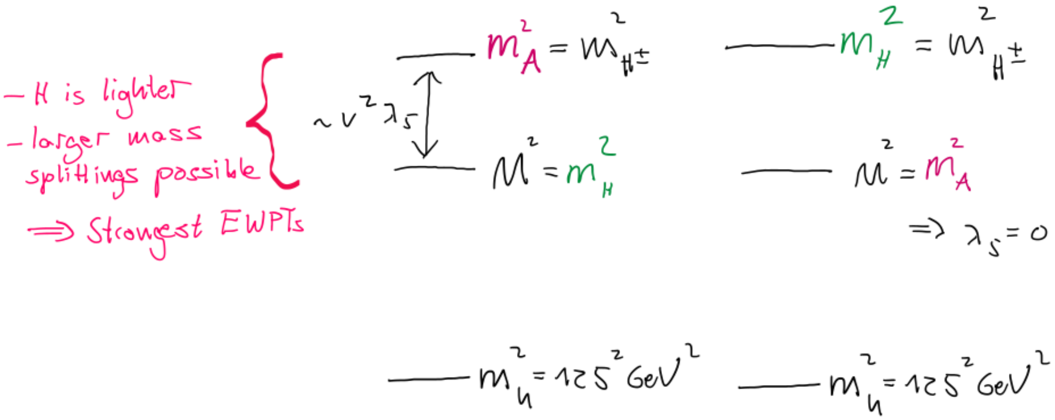

2HDM Higgs-boson spectrum

Non-decoupling scenarios for an EWPT after LHC Run 1 at 8 TeV:

Heatmaps: Valid | Strong EWPT

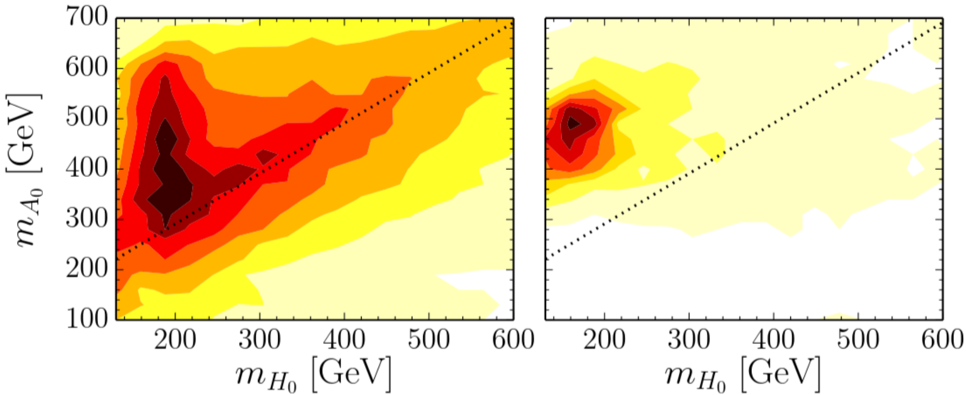

[Dorsch et al, hep-ph/1405.5537]

2HDM Higgs-boson spectrum

Non-decoupling scenarios for an EWPT during LHC Run 2 at 13 TeV:

$\tan\beta = 3, \quad \cos(\beta - \alpha) = 0, \quad 200\ \text{GeV} \leq m_H = M \leq 1000\ \text{GeV}, \quad 600\ \text{GeV} \leq m_A = m_{H^\pm} \leq 1000\ \text{GeV}$

$$\xi_c = \frac{v_c}{T_c}$$

$$\xi_n = \frac{v_n}{T_n}$$

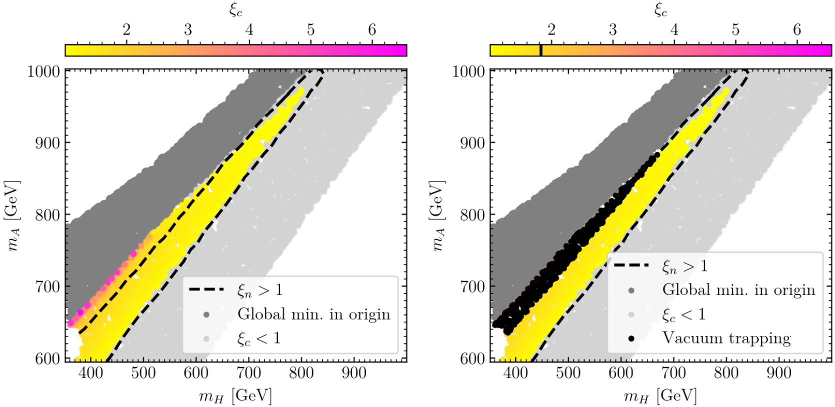

[TB, Heinemeyer, No, Olea-Romacho, Weiglein, hep-ph/2208.14466]

The smoking gun signal: projections

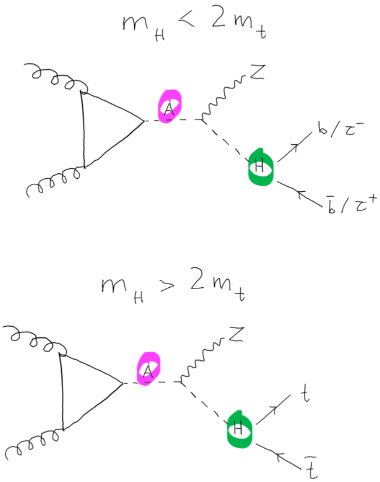

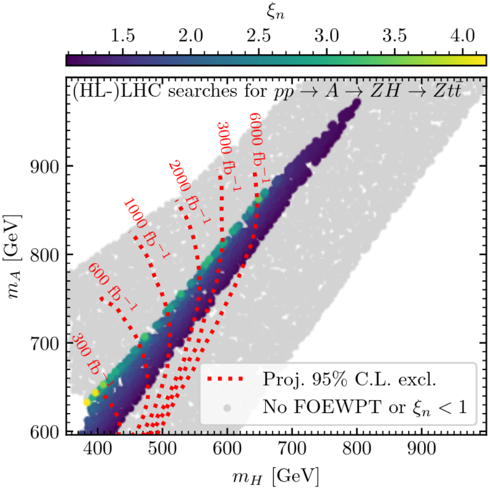

[TB, Heinemeyer, No, Olea-Romacho, Weiglein, hep-ph/2208.14466]

The smoking gun signal: Run 2 results

ATLAS: semi-leptonic channel

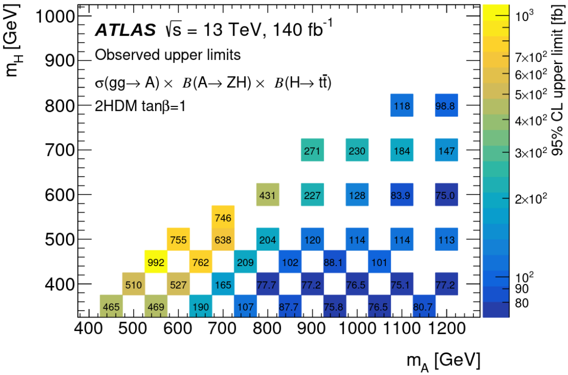

[ATLAS, hep-ex/2311.04033]

The smoking gun signal: Run 2 results

ATLAS: semi-leptonic channel

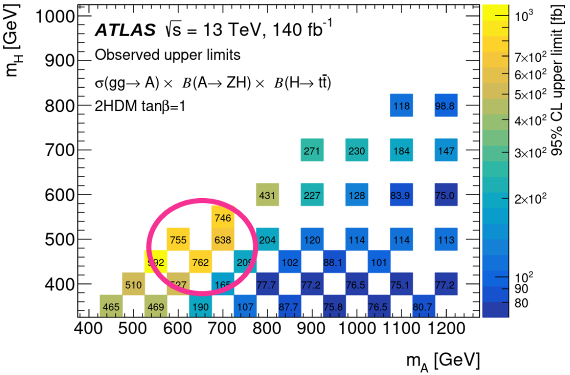

[ATLAS, hep-ex/2311.04033]

Impact on 2HDM

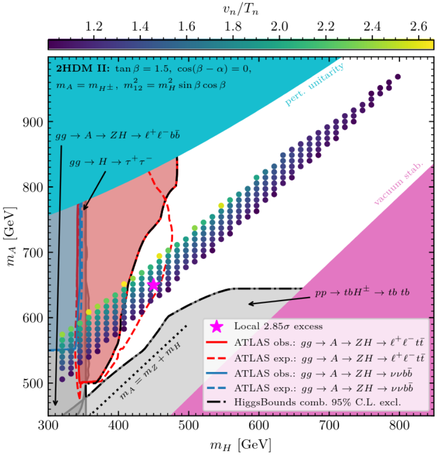

[TB, Heinemeyer, No, Radchenko, Olea-Romacho, Weiglein, hep-ph/2309.17431]

The smoking gun signal: Run 2 results

ATLAS: semi-leptonic channel

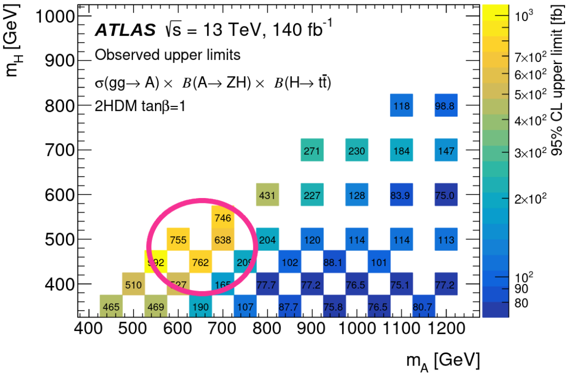

[ATLAS, hep-ex/2311.04033]

Impact on 2HDM

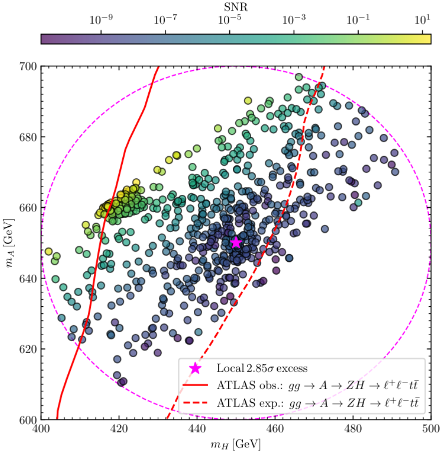

[TB, Heinemeyer, No, Radchenko, Olea-Romacho, Weiglein, hep-ph/2309.17431]

The smoking gun signal: Run 2 results

CMS: fully hadronic channel

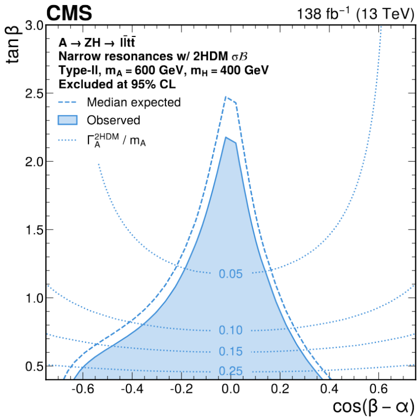

[CMS, hep-ex/2412.00570]

Impact on 2HDM

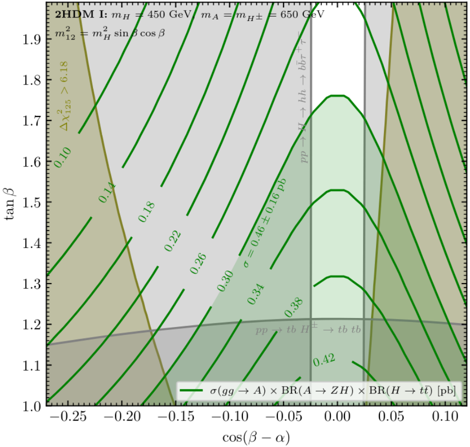

[TB, Heinemeyer, No, Radchenko, Olea-Romacho, Weiglein, hep-ph/2309.17431]

The smoking gun signal: our proposal

The $A \to ZH \to Zt\bar{t}$ signature is the most promising way to test so far unexplored 2HDM parameter space regions that predict a strong EWPT at the LHC

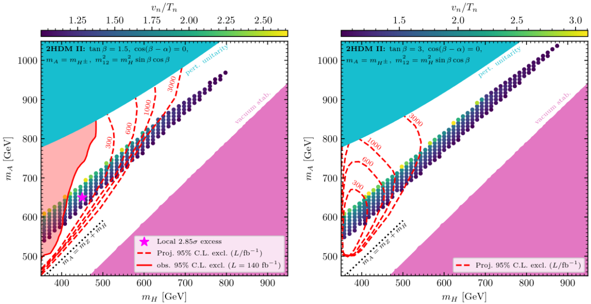

[TB, Heinemeyer, No, Radchenko, Olea-Romacho, Weiglein, hep-ph/2309.17431]

But current analyses techniques employed by ATLAS and CMS have an important limitation: no distinction possible between $A \to ZH$ and $H \to ZA$ signals

The smoking gun signal: our proposal

The $A \to ZH \to Zt\bar{t}$ signature is the most promising way to test so far unexplored 2HDM parameter space regions that predict a strong EWPT at the LHC

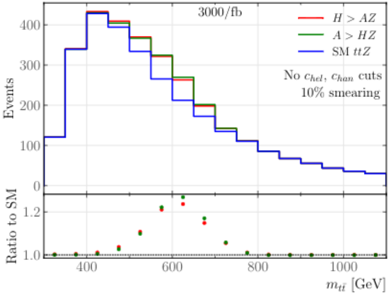

Use $t\bar{t}$ spin correlations in $Zt\bar{t}$ final state to distinguish between the two signals and to increase experimental sensitivity

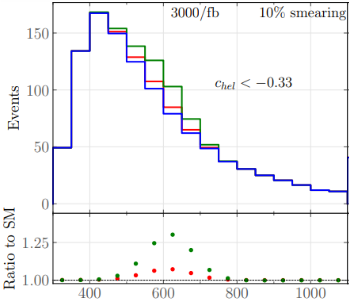

[F. Arco, TB, P. Stylianou, G. Weiglein, 2502.03443]

But current analyses techniques employed by ATLAS and CMS have an important limitation: no distinction possible between $A \to ZH$ and $H \to ZA$ signals

Top-quark spin correlations and angular variables

Lifetime of top quarks: $\tau = 0.5 \cdot 10^{-25}$ s $\rightarrow$ Decays before hadronization and spin de-correlation

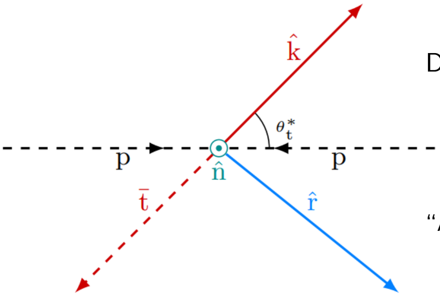

Spin density matrix of $t\bar{t}$ sub-system:

$$R \propto A\,\mathbb{1} \otimes \mathbb{1} + B_i^+ \sigma^i \otimes \mathbb{1} + B_i^- \mathbb{1} \otimes \sigma^i + C_{ij}\sigma^i \otimes \sigma^j$$

Differential cross section:

$$\frac{1}{\sigma}\frac{d\sigma}{d\cos\theta_{\hat{a}}^+ \, d\cos\theta_{\hat{b}}^+} = \frac{1}{4}\left(1 + B_{\hat{a}}^+ \cos\theta_{\hat{a}}^+ + B_{\hat{a}}^- \cos\theta_{\hat{a}}^- - C_{\hat{a}\hat{b}} \cos\theta_{\hat{a}}^+ \cos\theta_{\hat{b}}^-\right)$$

"Angles of leptons": $\cos\theta_{\hat{a}}^\pm = \pm \ell^\pm \cdot \hat{a}$

$\ell^\pm$ are direction of flights of leptons in their respective parent top-quark restframe, and $\hat{a} \in \{\hat{k}, \hat{r}, \hat{n}\}$

$$c_{hel} = -\cos\theta_{\hat{k}}^+ \cos\theta_{\hat{k}}^- - \cos\theta_{\hat{r}}^+ \cos\theta_{\hat{r}}^- - \cos\theta_{\hat{n}}^+ \cos\theta_{\hat{n}}^- = \hat{\ell}_t^+ \cdot \hat{\ell}_{\bar{t}}^-$$

$$c_{han} = \cos\theta_{\hat{k}}^+ \cos\theta_{\hat{k}}^- - \cos\theta_{\hat{r}}^+ \cos\theta_{\hat{r}}^- - \cos\theta_{\hat{n}}^+ \cos\theta_{\hat{n}}^-$$

Further reading e.g.: c_{hel}: [Bernreuther et al, 1508.05271], c_{han}: [CMS-PAS-HIG-22-013], $Zt\bar{t}$ SM: [Ravina et al, 2106.09690]

Top-quark spin correlations and angular variables

$$c_{hel} = -\cos\theta^+_{\hat{k}}\cos\theta^-_{\hat{k}} - \cos\theta^+_{\hat{r}}\cos\theta^-_{\hat{r}} - \cos\theta^+_{\hat{n}}\cos\theta^-_{\hat{n}} = \hat{\ell}^+_t \cdot \hat{\ell}^-_{\bar{t}}$$

$$c_{han} = \cos\theta^+_{\hat{k}}\cos\theta^-_{\hat{k}} - \cos\theta^+_{\hat{r}}\cos\theta^-_{\hat{r}} - \cos\theta^+_{\hat{n}}\cos\theta^-_{\hat{n}}$$

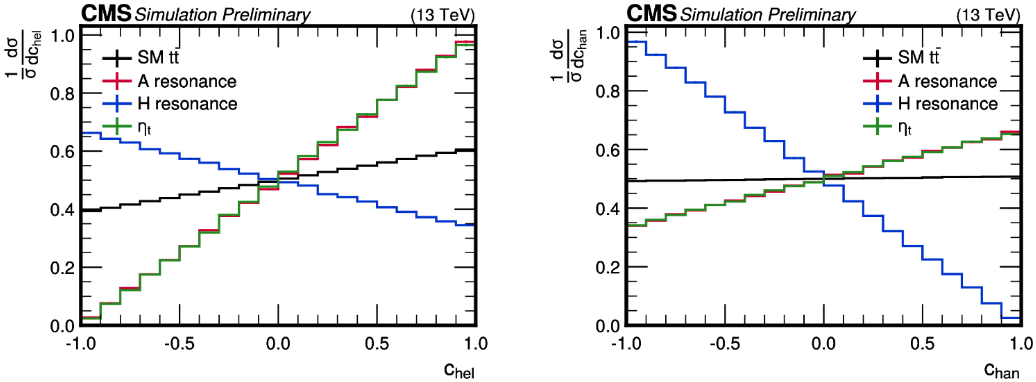

[CMS-PAS-HIG-22-013]

Top-quark spin correlations and angular variables

$$c_{hel} = -\cos\theta^+_{\hat{k}}\cos\theta^-_{\hat{k}} - \cos\theta^+_{\hat{r}}\cos\theta^-_{\hat{r}} - \cos\theta^+_{\hat{n}}\cos\theta^-_{\hat{n}} = \hat{\ell}^+_t \cdot \hat{\ell}^-_{\bar{t}}$$

$$c_{han} = \cos\theta^+_{\hat{k}}\cos\theta^-_{\hat{k}} - \cos\theta^+_{\hat{r}}\cos\theta^-_{\hat{r}} - \cos\theta^+_{\hat{n}}\cos\theta^-_{\hat{n}}$$

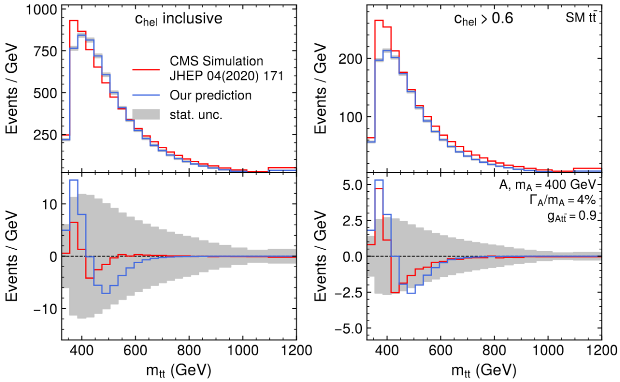

[Anuar, Biekötter, TB, Grohsjean, Heinemeyer, Jeppe, Schwanenberger, Weiglein, 2404.19014]

Monte Carlo simulation: Signal

$$gg \to \begin{pmatrix} A \\ H \end{pmatrix} \to \begin{pmatrix} ZH \\ ZA \end{pmatrix} \to Z\,t\bar{t} \to \ell^+\ell^-\, b\bar{b}\ell^+\ell^-\nu_\ell\bar{\nu}_\ell$$

- $gg \to A/H$ cross sections simulated at LO with MadGraph5_aMC@NLO
- LO Agg/Hgg vertices implemented in UFO with FeynRules including p^2-dependence:

$$\mathcal{L} \supset \frac{\alpha_S}{8\pi v}\left[\mathcal{F}_H(\tau) H G^a_{\mu\nu} G^{a\mu\nu} + i\mathcal{F}_A(\tau) A G^a_{\mu\nu} \widetilde{G}^{a\mu\nu}\right], \quad \tau = \frac{\hat{s}}{4m_t^2}$$

- NNLO QCD K-factor from HiggsTools/SusHi
- Decays $A/H \to t\bar{t}$ and $A \to ZH/H \to ZA$ from:

$$\mathcal{L} \supset -\frac{m_t}{v t_\beta}\bar{t}(H + iA\gamma_5)t - \frac{e}{2 s_W c_W}(H\partial_\mu A - A\partial_\mu H)Z^\mu$$

- Total width of heavier resonance includes NLO QCD and off-shell corrections from HDECAY

Background, cuts and efficiency factors

The main **background** in the fully leptonic channel is $pp \to Zt\bar{t}$ production:

- Simulated at LO with MadGraph5_aMC@NLO (leptonic decays: $t \to b\ell\nu_\ell$ and $Z \to \ell^+\ell^-$)
- Background normalization factor to obtain the same number of total background events as ATLAS in their measurement of SM $Zt\bar{t}$ production [2312.04450] (which includes additional minor backgrounds)

Cuts following ATLAS measurement of SM $Zt\bar{t}$ production [2312.04450]:

- Selected leptons are required to have $p_T(\ell) > 10$ GeV, $|\eta(\ell)| < 2.5$
- We require two pairs of OSSF leptons, with the leading lepton having $p_T(\ell) > 27$ GeV
- One lepton pair with invariant mass $m_{\ell\ell}$ close to m_Z: $|m_Z - m_{\ell\ell}| < 20$ GeV
- We require at least two b-jets with $p_T(j) > 25$ GeV and $|\eta(j)| < 2.5$

Efficiency factors to better simulate real experimental analysis:

- 10% gaussian smearing (for HL-LHC) to simulate detector response
- Efficiency factor of $(0.7)^2$ for b-tagging of jets
- Efficiency factor of 0.9 to account for reconstruction of top quarks

[F. Arco, TB, P. Stylianou, G. Weiglein, 2502.03443]

Results: $m_{t\bar{t}}$ distributions

Without angular variables sensitive to $t\bar{t}$ spin correlations:

$A \to ZH$ (no smearing)

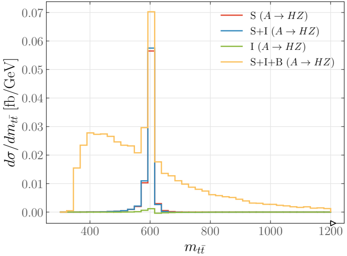

$H \to ZA$ (no smearing)

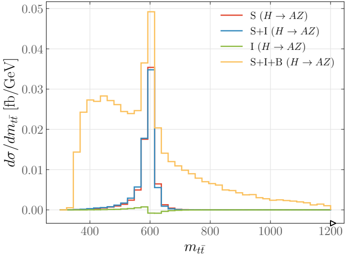

HL-LHC (10% smearing)

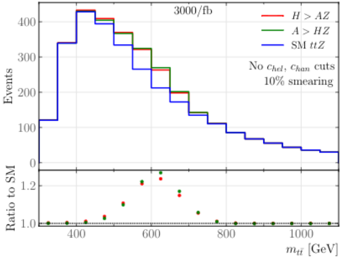

The two signals would be completely undistinguishable even after the full high-lumi Run of the LHC

[F. Arco, TB, P. Stylianou, G. Weiglein, 2502.03443]

Results: Angular distributions

Binning events in c_{hel} and c_{han}: (a.u.: arbitrary units)

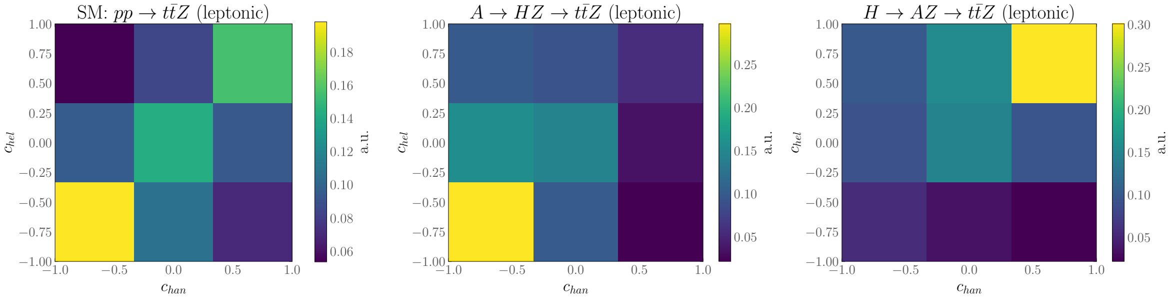

The two signals are potentially distinguishable:

$\Rightarrow$ $A \to ZH$ peaks in negative c_{hel} and c_{han} bin

$\Rightarrow$ $H \to ZA$ peaks in positive c_{hel} and c_{han} bin

[F. Arco, TB, P. Stylianou, G. Weiglein, 2502.03443]

Results: benchmark scenario at the HL-LHC

We define two 2HDM parameter points with same total cross section: $\mathrm{BP}_{H\to ZA}$ and $\mathrm{BP}_{A\to ZH}$

	$\mathrm{BP}_{H\to ZA}$	$\mathrm{BP}_{A\to ZH}$
$\tan\beta$	1.14	1.50
$\cos(\beta-\alpha)$	0	0
m_h/GeV	125	125
m_H/GeV	800	600
m_A/GeV	600	800
$m_{H^\pm}/\mathrm{GeV}$	800	800
M/GeV	600	600
$\mathrm{BR}(H\to t\bar{t})$	71%	99%
$\mathrm{BR}(A\to t\bar{t})$	99%	63%
$\mathrm{BR}(H\to ZA)$	29%	–
$\mathrm{BR}(A\to ZH)$	–	37%
Γ_H/m_H	4.3%	1.5%
Γ_A/m_A	3.5%	3.3%
$\sigma(gg\to H)/\mathrm{pb}$	0.35	0.89
$\sigma(gg\to A)/\mathrm{pb}$	2.43	0.27

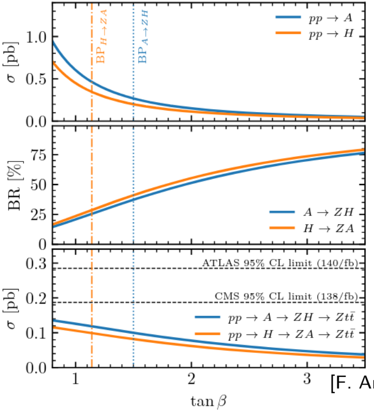

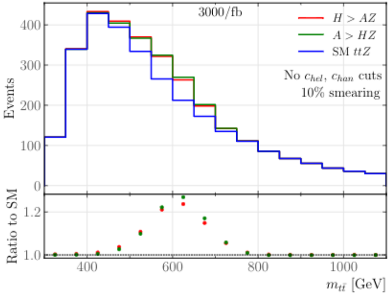

[F. Arco, TB, P. Stylianou, G. Weiglein, 2502.03443]

Results: benchmark scenario at the HL-LHC

$m_{t\bar{t}}$ distribution in different c_{hel} bins:

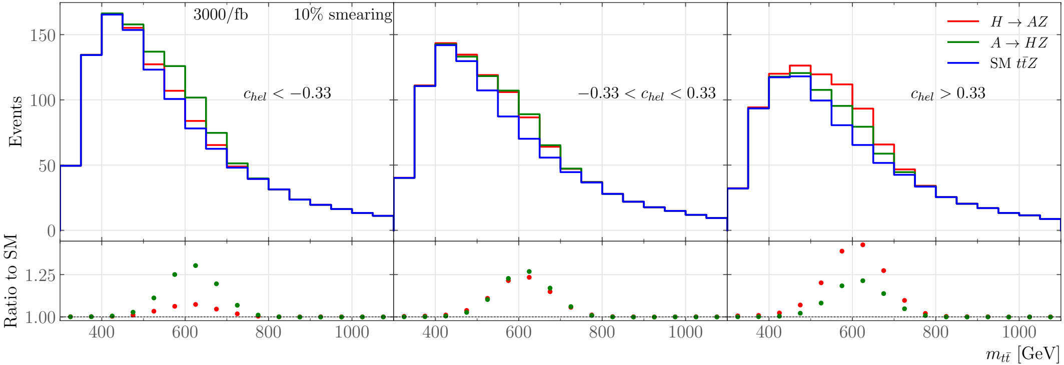

[F. Arco, TB, P. Stylianou, G. Weiglein, 2502.03443]

Results: benchmark scenario at the HL-LHC

$m_{t\bar{t}}$ distribution in different c_{han} bins:

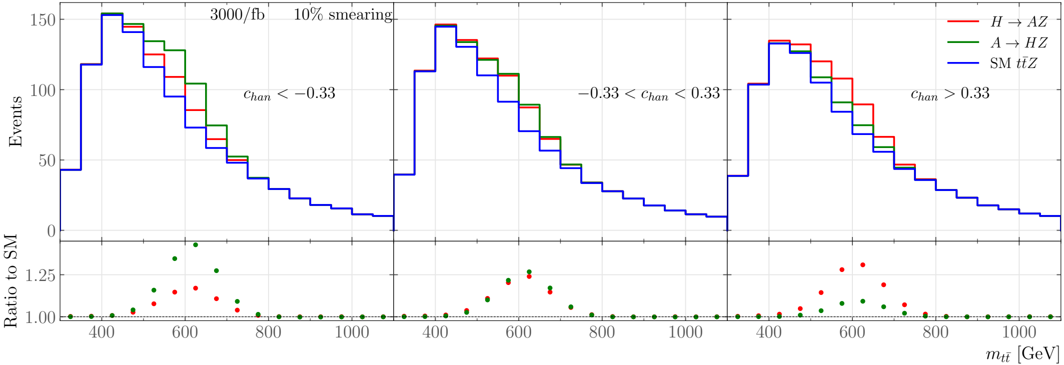

[F. Arco, TB, P. Stylianou, G. Weiglein, 2502.03443]

Results: benchmark scenario at the HL-LHC

Significances Z: binning only in c_{hel} or in c_{chan} — Without c_{hel} and c_{chan}: $Z < 6$

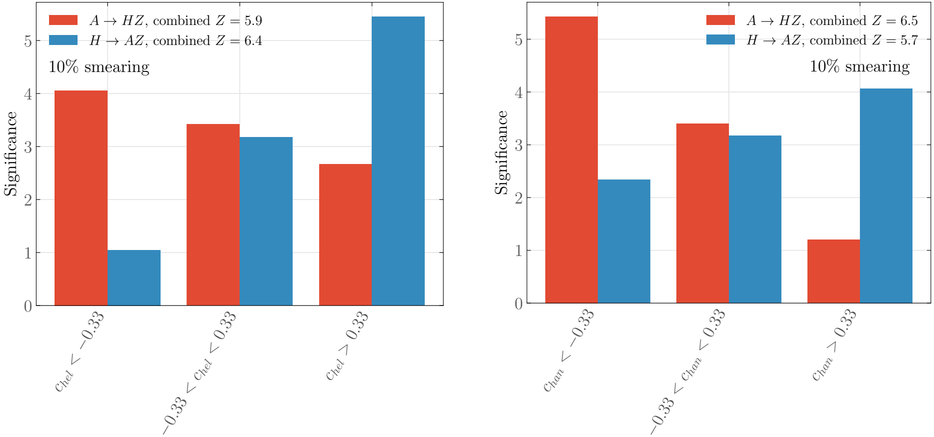

[F. Arco, TB, P. Stylianou, G. Weiglein, 2502.03443]

Results: benchmark scenario at the HL-LHC

Significances Z: binning both in c_{hel} or in c_{han}

Without c_{hel} and c_{han}: $Z < 6$

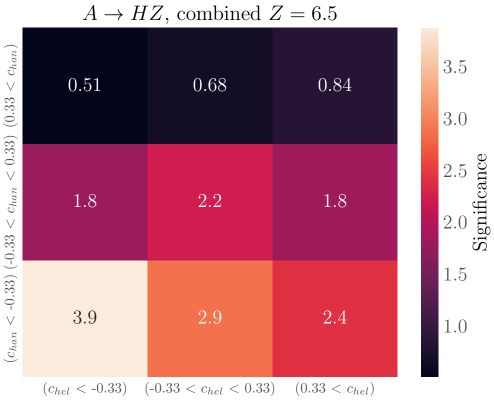

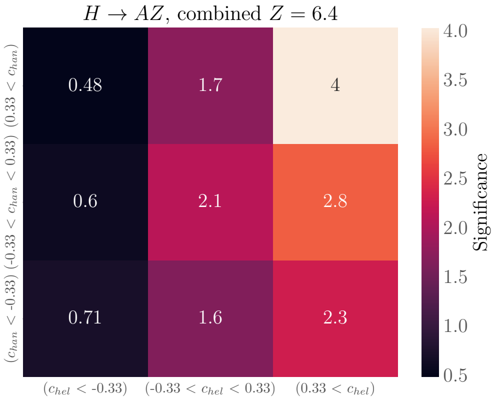

[F. Arco, TB, P. Stylianou, G. Weiglein, 2502.03443]

Summary

LHC Run 2 started probing models for EWPT with new physics above the $m_{t\bar{t}}$ threshold.
$\rightarrow$ $t\bar{t}+X$ final states increasingly important

At HL-LHC integrated luminosity is expected to increase by a factor of about 10, but better statistics will only get you so far.
$\rightarrow$ Improve techniques and exploit angular information

We showed in an explicit example how top-quark spin correlations can be utilised to further increase experimental sensitivity in a smoking-gun signature for a strong EWPT.

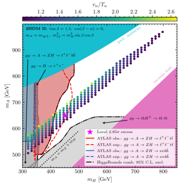

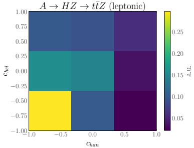

Thanks!

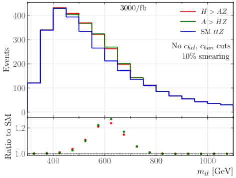

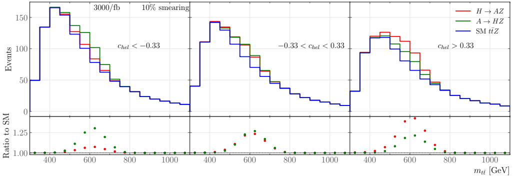

Exclusion regions from smoking gun: Type I/II

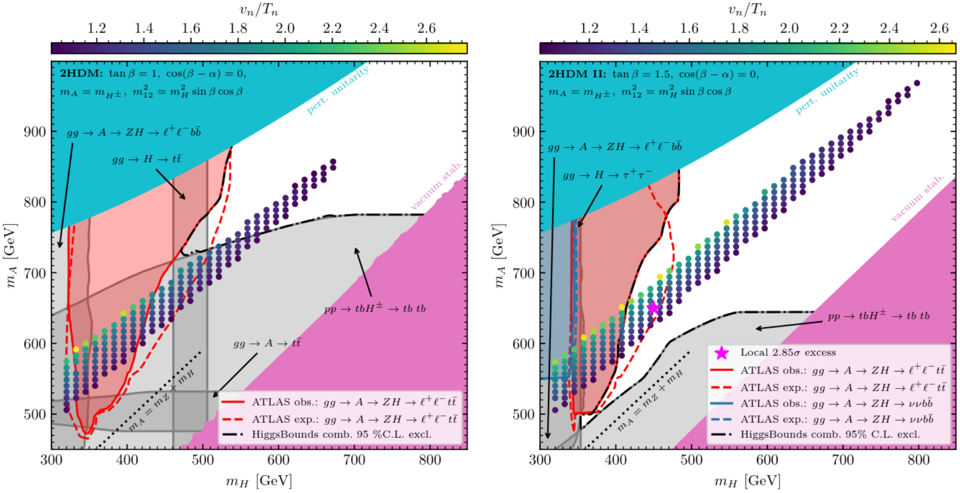

[TB, Heinemeyer, Olea-Romacho, No, Radchenko, Weiglein, 2309.17431]

Exclusion regions from smoking gun: Type IV

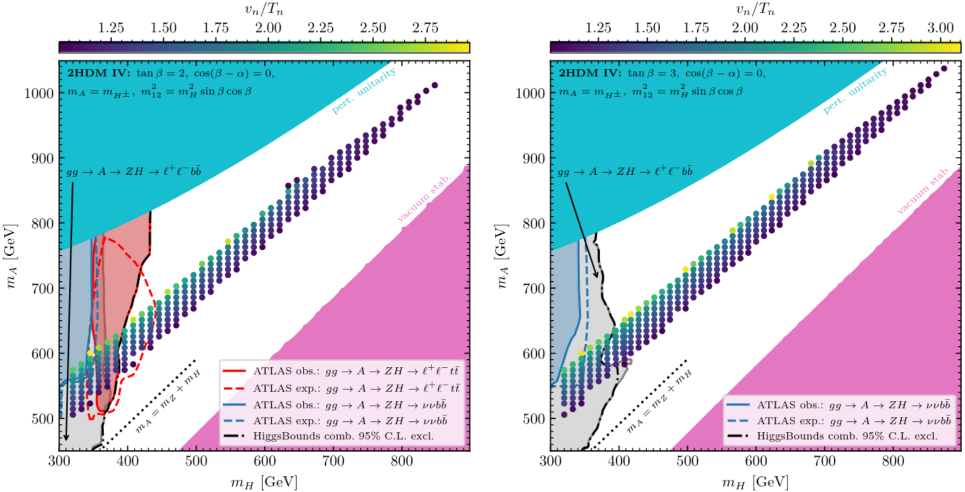

[TB, Heinemeyer, Olea-Romacho, No, Radchenko, Weiglein, 2309.17431]

EW symmetry non-restoration

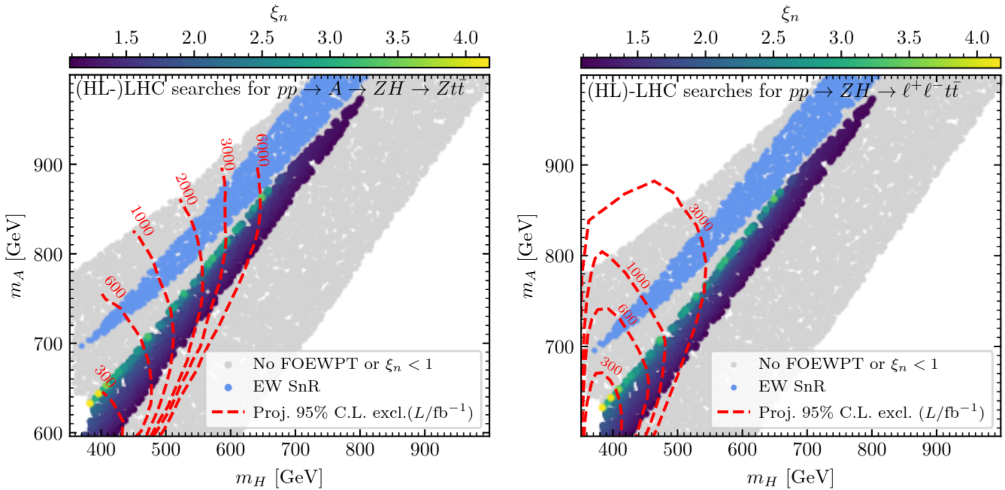

[TB, Heinemeyer, Olea-Romacho, No, Radchenko, Weiglein, 2309.17431]

UV cut-off, vacuum stability and h125 self-coupling

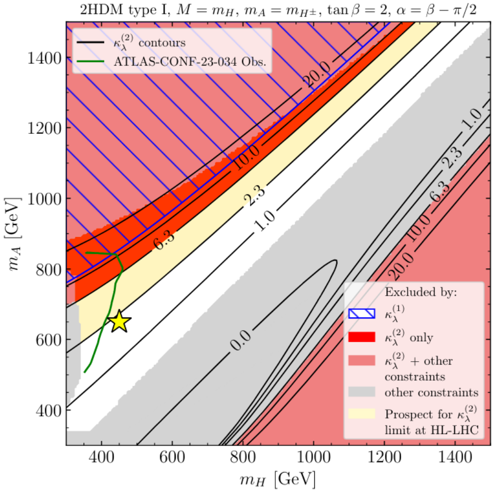

[Bahl, Braathen, Weiglein, 2310.20664]

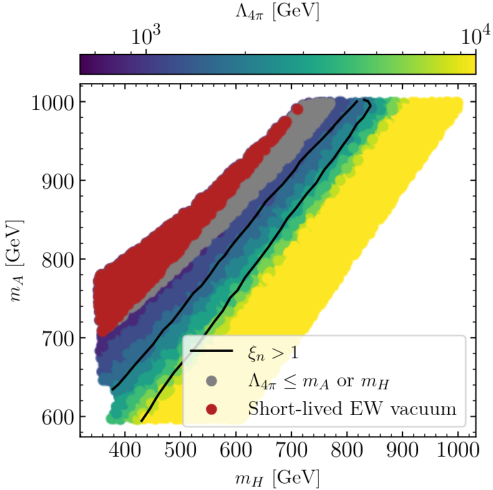

[TB, Heinemeyer, Olea-Romacho, No, Weiglein, 2208.14466]

EWPT and GW as collider targets

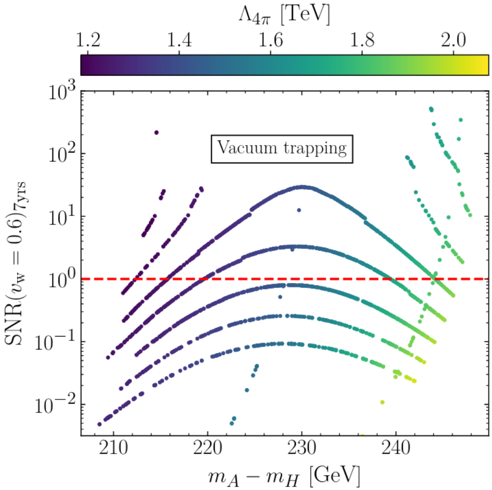

[TB, Heinemeyer, Olea-Romacho, No, Weiglein, 2208.14466]

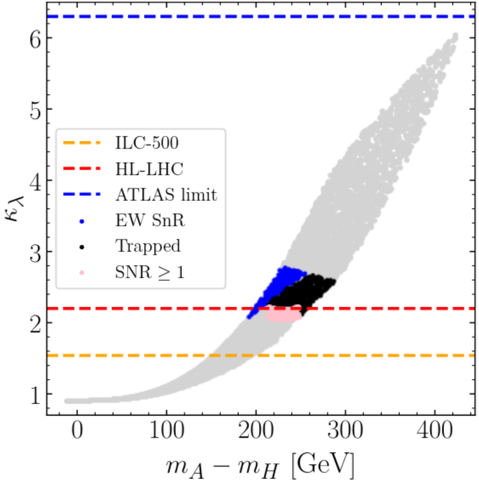

[TB, Heinemeyer, Olea-Romacho, No, Weiglein, 2208.14466]

EWPT, GW and h125 self-coupling

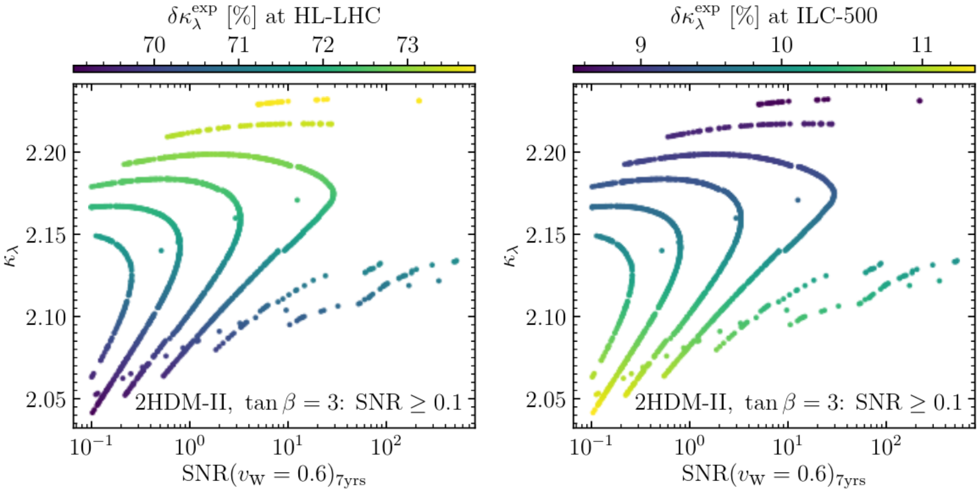

[TB, Heinemeyer, Olea-Romacho, No, Weiglein, 2208.14466]

Box-diagram contributions and signal-signal interference

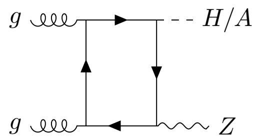

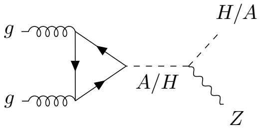

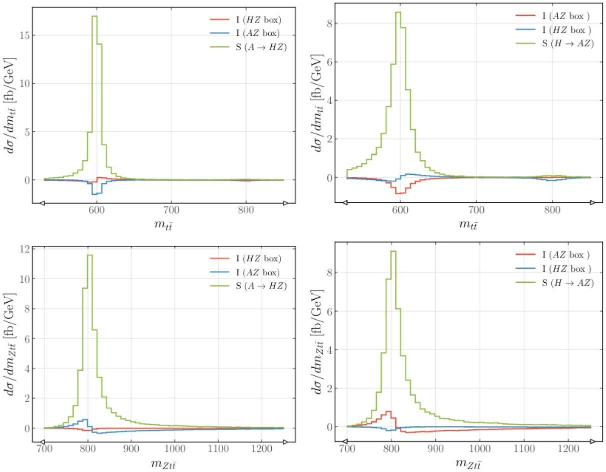

[TB, Heinemeyer, Olea-Romacho, No, Weiglein, 2208.14466]